Core Level Study of Alanine and Threonine

Vitaliy Feyer,*,† Oksana Plekan,†,‡ Robert Richter,† Marcello Coreno,§ Kevin C. Prince,†,∥ and Vincenzo Carravetta⊥

Sincrotrone Trieste, Area Science Park, I-34012 Basovizza (Trieste), Italy, CNR-IMIP, Montelibretti, Rome, I-00016 Italy, Laboratorio Nazionale TASC, CNR-INFM, 34012 Trieste, Italy, and CNR-Institute of Chemical Physical Processes, Via Moruzzi 1, 56124 Pisa, Italy

Received: April 7, 2008; Revised Manuscript Received: June 3, 2008

Core level X-ray photoemission spectra (XPS) and near edge X-ray absorption fine structure (NEXAFS) spectra of alanine and threonine in the gas phase have been measured at the carbon, nitrogen, and oxygen K edges and interpreted in the light of theoretical calculations. For the computations, a set of approximations is made which allows sufficiently accurate calculations of several conformers to be performed in reasonable computing time. The accuracy has been checked by comparing results obtained for proline to our previous, higher level calculations. The photoemission spectra at the carbon and oxygen edges are assigned and compared. The nitrogen 1s photoemission peaks show anomalous broadening which we relate to the populations and types of conformers. The carbon K-edge NEXAFS spectra of alanine and threonine are compared with our previous data on glycine and resonances assigned accordingly. The nitrogen K-edge NEXAFS spectra of alanine and threonine do not show measurable effects due to the population of conformers, in contrast to the photoemission results. At the oxygen K edge, the spectra of these amino acids are similar with two prominent peaks assigned to transitions of O 1s electrons from the oxo and hydroxyl groups to vacant π^* and σ^* orbitals and additional intensity for threonine due to the second OH group. Conformer effects are observable in photoemission but appear to be more difficult to resolve in photoabsorption. We explain this by energetic shifts of opposite sign for the core hole states and unoccupied orbitals, which causes partial cancelation in NEXAFS but not in photoemission.

1. Introduction

Biomolecules in the gas phase, such as DNA bases, amino acids, and peptides, have been the subject of a great number of theoretical and experimental investigations due to their biochemical significance. Their study in the absence of solvents allows a detailed understanding of their structure and dynamics and the distinction between intrinsic properties and those due to interaction with the environment. The considerable recent progress in experimental and theoretical methods has made it possible to study such low-density targets.[1] These studies provide important information about the details of geometrical and electronic structure.

In the past few years, there has been growing interest in characterization of biologically relevant systems by synchrotron radiation. Core level spectroscopy can provide insight into molecular electronic structure, and synchrotron radiation is an excellent source for photoemission and photoabsorption, particularly near edge X-ray absorption fine structure (NEXAFS). Amino acids studied by photoemission include glycine,[2–4] alanine,[5] methionine, and proline.[3,4] An attempt to study threonine[5] was not successful due to thermal decomposition of the sample. Theoretical calculations of core level spectra include calculations for glycine,[6] alanine,[5] and our own work.[3,4]

The soft X-ray technique of NEXAFS spectroscopy is a powerful tool for investigation of the electronic structure of organic molecules.[7] Theoretical calculations of the carbon, nitrogen, and oxygen K-edge NEXAFS spectra of amino acids have been reported.[8–14] Experimental NEXAFS spectra of amino acids have been reported in different phases, such as adsorbed on surfaces, dissolved in liquids, and in the gas phase.[15–22] The NEXAFS spectra of proline, lysine, and diglycine in solution have also been measured as a function of pH by Messer et al.[23] The spectral features were assigned by comparison with the previously reported spectrum of aqueous glycine[24] and calculated spectra of isolated amino acids and hydrated amino acid clusters. The solid-phase nitrogen K-edge spectrum was nearly identical to the solution spectra measured at low and moderate pH, while the basic solution spectra were similar to the gas-phase spectra.[24] In acid solution and the solid state amino acids are generally in the zwitterionic form, whereas in the gas phase they are generally not ionized.

Some amino acids have been examined in the gas phase by electron energy loss spectroscopy (EELS), which is equivalent to NEXAFS spectroscopy for the conditions used. Glycine and some related compounds have been investigated by Gordon et al.[25] at the carbon, nitrogen, and oxygen K edges, while Cooper et al.[26] reported C 1s EELS spectra of gaseous glycine, glycylglycine, alanine, and phenylalanine. The gas-phase absorption spectra of L-alanine and L-proline (N and O edges) have been measured by Marinho et al.,[27] and that of alanine has also been studied by Morita et al. [28] (C, N, and O edges). Recently we reported the gas-phase photoabsorption spectra of glycine, methionine, and proline at the C, N, and O K edges.[29] In

* To whom correspondence should be addressed. Phone: +39 0403758287. Fax: +390403758565. E-mail: vitaliy.feyer@elettra.trieste.it.
† Sincrotrone Trieste.
‡ Permanent address: Institute of Electron Physics, 88017 Uzhgorod, Ukraine.
§ CNR-IMIP.
∥ Laboratorio Nazionale TASC.
⊥ CNR-Institute of Chemical Physical Processes.

10.1021/jp803017y CCC: $40.75
Published on Web 08/01/2008

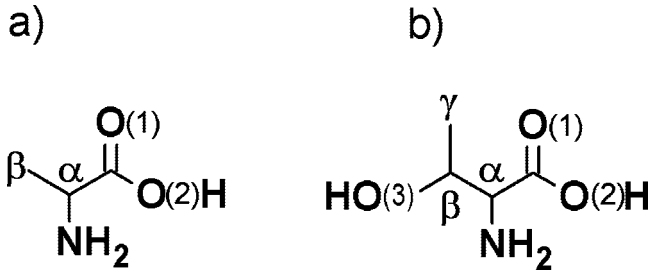

Figure 1. Schematic structures of (a) alanine and (b) threonine.

addition, the N and C 1s spectra of lysine in the liquid state have been reported.[30]

NEXAFS traditionally provides electronic structure data, and for information about the overall shape or conformation of amino acids we must turn to vibrational and microwave spectroscopy. Stepanian et al.[31] measured the infrared spectra of matrix-isolated alanine and carried out calculations to interpret their data. They observed two conformers of alanine labeled I and IIa: conformer I is characterized by an asymmetric $NH_2\cdots O{=}C$ hydrogen bond, while conformer IIa contains an $OH\cdots N$ hydrogen bond. Their calculations predicted that four conformers are populated at the evaporation temperature of 429 K, and they explained the observation of only two species as an effect of cooling by the noble-gas matrix. They suggested that the energy barriers between the observed and predicted conformers were sufficiently small for them to convert but sufficiently large that conformers I and IIa could not convert. In contrast to these results, a recent infrared vibrational study[32] of alanine vapor did not find any evidence for hydrogen-bonded conformers at 520 K.

Blanco et al.[33] recently analyzed the rotational spectrum of laser-ablated, jet-cooled alanine and determined the structural parameters and populations of the two conformers I and IIa. They also predicted that four conformers are populated at 298 and 498 K and explained the observation of only two species as an effect of cooling and interconversion.

We are not aware of experimental studies of threonine in the gas phase or isolated in low-temperature matrices. However the recent calculations of ref 34 indicate that many low-energy conformers are populated at laboratory temperatures.

In the present paper, we report the experimental photoemission and NEXAFS spectra at the three core edges (C, N, O) of alanine and threonine in the gas phase and report new insights into their electronic structure in the light of our calculations. Alanine is one of the simplest amino acids and is aliphatic, while threonine is an amino acid containing a hydroxyl group. The schematic structures of these compounds and the conformers we modeled are shown in Figures 1, 2, and 3. The conformers are labeled as follows.[34,35] The carbon atom bonded to the amino group is labeled Cα, and the other carbon atoms in the side chain are labeled sequentially with Greek subscripts, while the carboxylic carbon atom is not labeled. The oxo oxygen atom is denoted O(1), the hydroxyl oxygen atom in the carboxylic groups is O(2), and the additional oxygen atom in threonine is marked O(3).

An issue we address in this paper is the extent to which we can gain information from core level spectroscopy about amino acid conformers present in the vapors. We compare photoemission and photoabsorption both theoretically and experimentally and examine the sensitivity of these spectroscopic techniques to conformational differences.

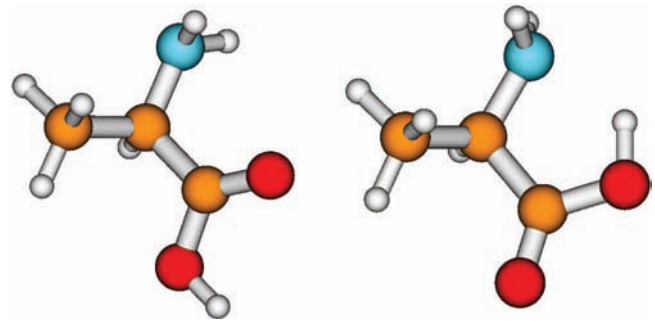

Figure 2. Structure of conformers I and IIa of alanine. The color of the spheres indicates the atoms: white, hydrogen; orange, carbon; red, oxygen; blue, nitrogen. (Left) I, $NH_2\cdots O{=}C$ hydrogen bonding. (Right) IIa, $COH\cdots N$ hydrogen bonding.

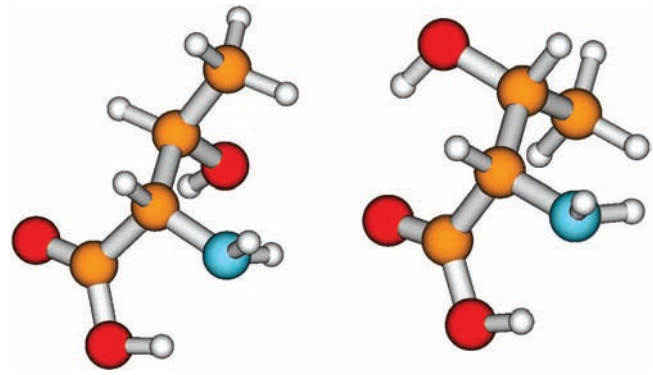

Figure 3. Structure of conformers 1 and 2 of threonine. (Left) 1, $COH\cdots N$, $NH_2\cdots O(3)H$ hydrogen bonding. (Right) 2, $COH\cdots N$, $O(3)H\cdots O{=}C$ hydrogen bonding.

2. Experimental Section

The measurements were performed at the gas-phase photoemission beamline, Elettra, Trieste.[36] For core level photoemission, the total resolution of the photons and analyzer was estimated to be 0.32, 0.46, and 0.78 eV at $h\nu = 382$ (C 1s), 495 (N 1s), and 628 eV (O 1s), respectively. The energy scale was calibrated by reference to the following core levels and gases: 297.6 eV (C 1s, CO_2), 409.9 eV (N 1s, N_2),[38] 541.3 eV (O 1s, CO_2).[38] The resolution was checked by measuring photoemission from the core levels of these reference samples. For the O 1s level of CO_2, which shows substantial structure, we used the parameters of Hatamoto et al.[39] to fit our spectra with our resolution as a free parameter. Some spectra were also taken at lower total resolution for direct comparison with our earlier results: 0.57 and 0.59 eV for C 1s and N 1s, respectively.

The NEXAFS spectra were recorded by collecting the ion yield signal using a channel electron multiplier placed close to the ionization region. In the geometry used, some energetic ions may be lost, so the ion yield is partial rather than total. The spectra at the carbon, nitrogen, and oxygen K edges were normalized to the photon flux measured by a photodiode. The energy scales of the spectra were calibrated by taking simultaneous spectra of the samples and a calibrant gas introduced into the experimental chamber. The NEXAFS spectra were recorded with energy resolution of 0.07, 0.06, and 0.10 eV at the C, N, and O K edges, respectively. The energies were calibrated to the following resonances: 290.77 eV (C 1s $\rightarrow \pi$, CO_2),[40] 400.87 eV (N 1s $\rightarrow \pi$, N_2),[41] 535.4 eV (O 1s $\rightarrow \pi$, CO_2).[42]

Alanine and threonine, purchased from Sigma Aldrich in the form of crystalline powders with a minimum purity of 99%,

were used without further purification and sublimated. A few grams of powder of each amino acid were placed in a noncommercial, noninductively wound furnace equipped with a chromel/alumel thermocouple.[4] The evaporation temperatures were 423 K for alanine and 433 K for threonine, and the pressure in the chamber remained in the 10^{-8} mbar range during the experiments. Before the experiment, the samples were evaporated from the same furnace in another apparatus and photoionisation mass spectra were measured to check for purity and absence of thermal decomposition and determine the appropriate temperature for evaporation. During the experiment the sample quality was monitored by valence band photoemission. The peak energies of the spectra were similar to previously published He I spectra,[43] and no signs of thermal decomposition were observed (for example, time-dependent changes, presence of decomposition products such as water or carbon dioxide, change of color of the sample after the experiment, etc.).

3. Theoretical Section

Ab-initio calculations of the XPS and NEXAFS spectra were carried out in order to assign the main peaks of the experimental spectra and assess a possible conformational dependence of the core photoabsorption spectra similar to that which we reported for the photoemission spectrum of proline.[3] An accurate theoretical simulation of core excitation/ionization processes in molecules is still a difficult task to perform by the usual quantum chemical approaches because of a number of conceptual and technical problems essentially connected to the highly excited (hundreds of electronvolts above the ground state) character of the final states. The problems related to an accurate description of both electronic relaxation (a dominant effect in the ionization/excitation of core electrons) and electronic correlation are magnified in the case of molecules of medium (as in the present study) or large size.

Computational approaches have recently been proposed based on sophisticated propagator methods, which can be employed for the simulation of NEXAFS[44] and XPS[45] spectra. In the first case, a resonant-convergent first-order polarization propagator (CPP) approach, implemented in density functional theory, which makes it possible to directly calculate the X-ray absorption cross section at a particular frequency without explicitly addressing the excited states, was applied to the calculation of NEXAFS spectra of molecules as large as the guanine-cytosine and adenine-thymine base pairs. While this approach is efficient in providing a total photoabsorption profile whose accuracy depends only on the density functional employed, assignment of the individual spectral peaks is not straightforward, as will be discussed. This aspect, which is of course relevant in the interpretation of complex spectra, will require some improvements of the method for analysis of the computational data that, in principle, contain such detailed information.

In the second case a transition operator method combined with second-order, self-energy corrections to the electron propagator was proposed to calculate valence and core−electron binding energies by which a simulation of core photoemission spectra can be obtained. This approach has the additional advantage of describing at the same time electronic relaxation and correlation effects and appears promising from the point of view of applicability to large molecules. This is because the scaling factor of the computational effort with the size of the system is smaller than that of traditional Green function methods. However, the method has not been tested so far on large molecules, such as those considered in the simulation of NEXAFS spectra by the polarization propagator approach, and its practical applicability and accuracy for large molecules is still questionable.

In the present investigation, we preferred to employ state-specific approaches where the initial and final states are computed by taking into account fully the electronic relaxation but neglecting the electronic correlation that, in the present context of predicting chemical shifts related to different conformational geometries of a molecule, can reasonably be assumed to be a minor effect. Such a choice allows us to make an easier assignment of observed spectral features to specific aspects of the electronic and geometrical structures and also a direct comparison with our previous studies.[3,4]

The C, N, and O core ionization potentials of alanine and threonine were then computed by the Δ SCF procedure using the DALTON package[46] at the geometry of the ground-state optimized by a DFT/B3LYP[47] calculation using the GAMESS package.[48] The TZV[49] basis set was employed for geometry optimization, while for the description of the core ionization/excitation processes the Ahlrichs[50] basis set {C,N,O(10s,6p) → [6s,3p], H(4s) → [2]} was adopted, augmented with {5s, 5p, 5d} diffuse functions on the site of ionization/excitation, for a better description of the electronic relaxation and of the lowest virtual orbitals.

The vertical transition approximation was tested on four conformers of proline by comparison with the separate geometry and electronic optimization of the ground state and N(1s) hole state employed in our previous investigation.[3] A simple and efficient ab-initio method, widely applied to the simulation of NEXAFS spectra of large molecules, is the static exchange (STEX) approach.[51] It consists of a separate states calculation in which the ground state is approximated by the SCF wave function while the core excited state is approximated by the coupling of a relaxed target ionic state and an optimized excited orbital. This is one of the eigenvectors of a one-particle Hamiltonian that describes the motion of the excited electron in the static field of the remaining molecular ion corresponding to a specific relaxed core-hole state. In the STEX approximation, the electronic relaxation is then that of the core hole and the screening effect of the excited electron is neglected. It was early recognized that a main consequence of the STEX approximation is a compression of the energy scale of the calculated spectra to the ionization potential edge. In the present investigation we performed a full optimization of each final core excited-state separately in order to include the screening effect missing in the STEX approximation by RAS (restricted active space) MCSCF (multiconfigurational SCF)[46] calculations adopting the simplest representation of the final state, namely, a single excited singlet configuration. This approach can be practically applied only to a limited set of core excited states, while the STEX method is able to simulate the photoabsorption spectrum over a wide energy range covering also the electronic continuum. However, considering that our estimation of a possible conformational effect on the NEXAFS spectra of a complex molecule will focus only on the main peaks that can be well resolved experimentally and correspond to core excitations below the ionization threshold, the RAS calculations can be considered sufficient.

In our previous studies on proline[3] we ran calculations for a reasonable set of the most stable conformers of the molecule because, due to the relative structural rigidity of the pyrrole ring, the number of relevant conformers, four, is rather small.[35] This is not true for alanine[31] and threonine[34] where, due to the presence in the molecular structure of a long and flexible chain, the number of conformers with similar energy is so large as to

TABLE 1: N 1s Binding Energy of Four Conformers of Proline Computed by the ΔSCF Method in the Vertical Approximation (VA) Compared to Adiabatic (A) Values Obtained by Separate Geometry and Electronic Optimization of the Ground State and Core-Hole State and the Lowest Core Excitation Energy Computed in the Vertical Approximation (VA) by the RAS-MCSCF Method[a]

conformer	vertical binding energies (eV)	Δ_{12} (eV)	adiabatic binding energies (eV)	Δ_{12} (eV)	vertical excitation energy to LUMO (eV)	Δ_{12} (eV)
Proline_1a	405.51	0.88	405.71	1.0	401.95	−0.03
Proline_2a	404.63		404.71		401.98	
Proline_1a	405.50	0.86	405.67	0.99	401.96	−0.10
Proline_2b	404.64		404.68		402.06	

[a] For structures, see refs,[35,59] and.[60] Δ_{12} indicates the energy difference between conformers of type 1a and 2a or 1b and 2b for each type of excitation.

make a systematic simulation of the photoemission and photoabsorption spectra for a complete set of low-energy conformers simply unfeasible. We therefore selected for each of these molecules two conformers, whose structures are reported in Figures 2 and 3, that (similarly to the four proline conformers) are representative of different schemes for the internal hydrogen bonding at the origin of the chemical shift observed, or observable, in the spectra. The alanine conformers selected are those observed via matrix isolation and microwave spectra, and the threonine conformers are the two lowest energy forms, according to the total energy calculations of Zhang et al.[34] The theoretical analysis of only two conformers can be seen as a qualitative estimation of the dependence of the XPS and NEXAFS spectra of alanine and threonine on the molecular geometry.

4. Results

4.1. Vertical Approximation. In our previous experimental and theoretical study[3] of conformational effects in the N 1s photoemission spectrum of proline, simulations of the spectra of four low-energy conformers of proline, shown in Figure 3 of ref 3 were calculated theoretically by a ΔSCF procedure with separate geometry and electronic optimization of the ground state and of the core-hole state. Moreover, the vibronic photoemission profile was obtained from the set of Franck−Condon (FC) factors computed between the ground vibronic state and the different vibrational states of the final electronic core-hole state, taking into account the Duschinsky effect for transitions between vibrational states projected on different normal coordinate reference systems. This accurate and computationally expensive procedure allowed us to obtain a detailed theoretical photoemission band and, by comparison with the experimental data, prove that the two peaks distinguishable in the observed photoemission spectrum could not be traced to a complex structure of the vibrational band. Instead, they were unambiguously due to the contributions to the spectrum of different conformers of the molecule.

In the present investigation of conformational effects in the XPS and NEXAFS spectra of two other amino acids we tested a less computationally expensive approach that could possibly be applied also to larger molecules in future studies. For this purpose the ΔSCF procedure was applied in the vertical approximation (VA) at the optimized geometry of the ground state; Table 1 shows a comparison of the results obtained for four conformers of proline (see Figure 3 of ref 3 for structures) with the adiabatic core binding energies previously computed. Not only are the values of the VA ionization potentials rather close to the adiabatic values, but also their differences (Δ_{12}) for conformers of type 1 and 2 show a modest variation (about 10%) that does not affect our final conclusions. The VA was then adopted in all the following calculations of the XPS and NEXAFS spectra of alanine and threonine.

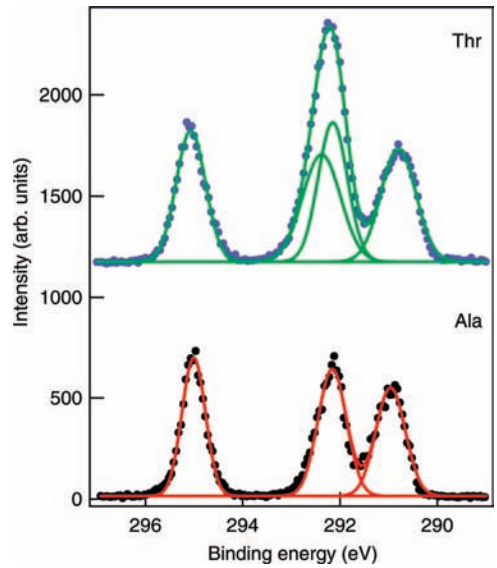

Figure 4. C 1s photoemission spectra of threonine (upper dotted curve) and alanine (lower dotted curve) together with fitted peaks: points, data; solid lines, fitted curves.

We also report in Table 1 the excitation energy from N 1s to the LUMO, obtained by the RAS-MCSF method in the VA, for the four conformers. The values of Δ_{12} of this quantity are much smaller than those predicted for the N 1s ionization potential. This is a first indication, confirmed by the calculations for alanine and threonine discussed in the following, that conformational effects on the photoabsorption spectrum are minor and that it may be difficult to observe them in a NEXAFS spectrum.

4.2. Photoemission of Alanine and Threonine. Figure 4 shows the carbon 1s photoemission spectra of alanine and threonine and peaks which have been fitted to the data assuming Gaussian line shapes. The numerical data are summarized in Table 2, and the intensities of the three peaks are equal within 13%. The cross-sections of the lines are expected to be approximately equal, but two effects may change the ratio of intensities. The excitation of satellites may transfer some of the oscillator strength out of the main lines to satellite lines, and the magnitude of this effect will be different for different core levels. Although the spectra are taken about 100 eV above threshold, extended X-ray absorption fine structure effects may change the cross section. The change is usually on the order of a few percent, but it has been shown recently that it can reach about 10% in some cases at this kinetic energy.[52] Thus, equal intensity within 13% is considered satisfactory.

The theoretical values in Table 2 have been obtained by the ΔSCF procedure applied in the VA at the optimized geometry of the ground state for the two geometries reported in Figure 2 (I and IIa, respectively) that correspond to the structures of the

TABLE 2: C 1s, N 1s, and O 1s Binding Energy for Alanine and Threonine

molecule	core level	binding energies (eV), ± 0.1 eV	fwhm of the Gaussian fit function (eV)	theoretical binding energies (eV) (I − IIa)	assignments	area
alanine	C 1s	291.0	0.71	291.5−291.8	Cβ	0.87
		292.2	0.68	293.0−293.3	Cα	1
		295.0	0.57	296.5−296.1	C (COOH)	0.91
	N 1s	405.2	0.66	405.4 (I)	CF2	0.78
		405.9	0.66	406.3 (IIa)	CF1	0.22
	O 1s	538.2	1.06	538.0−537.3	O(1)	0.88
		540.0	1.32	539.9−539.0	O(2)	1
threonine	C 1s	290.8	0.85	291.6−291.6	Cγ	0.97
		292.2	0.71	293.2−293.4	Cα	1
		292.4	0.92	293.4−293.3	Cβ	1
		295.1	0.71	296.3−296.5	C (COOH)	0.94
	N 1s	405.4	0.8	406.2 1	CF2	0.66
		405.9	0.8	406.6 2	CF1	0.34
	O 1s	538.4	1.18	537.5−537.7	O(1)	0.84
		538.7	1.41	538.6−538.0	O(3)	1
		540.1	1.46	539.2−539.5	O(2)	0.94

two most stable conformers of alanine.[31,33] Small but significant conformational effects on the C 1s binding energies are predicted (0.3−0.4 eV), which are however all less than the measured widths. The assignments follow from our computation and from previous studies of glycine;[2,4] alanine differs from glycine by possessing an additional methyl group, and as expected, there is an additional peak in the C 1s spectrum. These assignments agree with those of Powis et al.[5] Considering the approximations made, the predicted energies agree reasonably well with the experimental values with shifts in absolute energies of 0.6−1.3 eV.

Threonine contains one more carbon atom than alanine, Cβ, and the spectrum shows additional intensity at about the binding energy of the Cα atoms of glycine and alanine. It is chemically reasonable that the additional peak is due to Cβ as it is bonded to an electrophilic hydroxyl group, while Cα is bonded to an electrophilic amine group. The spectrum was fitted with four Gaussian peaks, whose energies, widths, and intensities were free parameters. The peak at 295.1 eV has almost exactly the same energy as the carboxylic C peak of alanine, as predicted by the calculation, and is so assigned. The measured width of the latter peak is 0.71 eV, compared with 0.57 eV for alanine. As stated above, the resolution was 0.32 eV, so subtraction in quadrature gives estimated intrinsic widths of 0.47 and 0.63 eV for alanine and threonine, respectively. The calculation suggests that this additional broadening is not due to conformational effects (predicted to be larger for alanine), so it could be due to vibrational broadening.

The Cα and Cβ peaks of threonine overlap and fitting suggests two peaks separated by about 0.2 eV. The calculation also predicts a difference of 0.1−0.2 eV for conformer 1 or 2. Following the calculation, we assign the lower binding energy peak (292.2 eV) to Cα, which places it at the same binding energy as the Cα atom of alanine.

The methyl Cγ peak at 290.8 eV has a slightly lower energy than the corresponding methyl Cβ peak of alanine, 291.0 eV. We attribute the shift to final state effects: threonine is slightly larger than alanine, so it can screen the core hole more effectively, lowering the binding energy. Initial state effects, due to charge withdrawal by the electronegative hydroxyl group (the second nearest neighbor of the Cγ atom), would be expected to produce a shift in the opposite direction. As in the case of alanine, the experimental and theoretical binding energies agree reasonably well with differences between theory and experiment of about 0.8−1.2 eV. We note that the theoretical differences of the C 1s binding energies between conformers are smaller for threonine, 0.2 eV on average, compared with 0.4 for alanine.

The nitrogen 1s spectra of alanine and threonine are shown in Figure 5. The spectrum of alanine was also taken at lower resolution (see Experimental Section) under the same conditions as in our previous studies to allow a direct comparison with glycine. We observe a distinct shoulder at higher binding energy and assign this to the presence of multiple conformer(s) as in the case of proline.[3] Threonine shows only a broad peak with no resolved structure. The measured N 1s line widths are significantly larger than those of glycine, and we (rather arbitrarily) fit the peaks with two Gaussian line shapes, assuming they have equal widths, and label them CF1 and CF2. This is intended to model the average IP of two groups of conformers rather than imply that only two conformers are present.

The results of the fit and calculations are summarized in Table 2. For alanine, we obtain experimentally two peaks separated by 0.7 eV. The calculation predicts that the two selected conformers have N 1s IPs separated by 0.9 eV. These experimental and theoretical results are strongly reminiscent of our results for proline, where we found that conformers with different hydrogen bonding (OH···N versus NH···O═C) gave

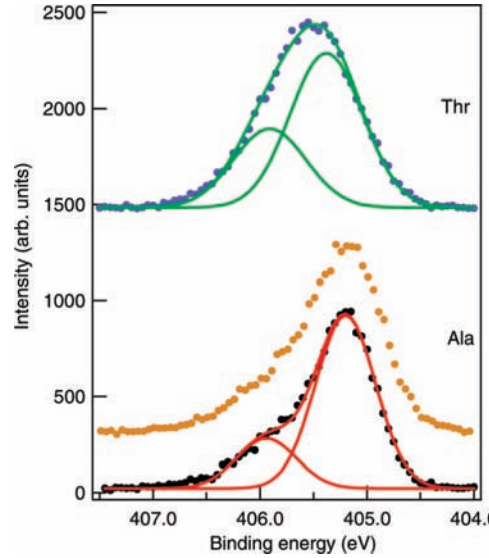

Figure 5. N 1s photoemission spectra of threonine (upper dotted curve), alanine at low resolution (middle dotted curve), and alanine at high resolution (lower dotted curve): points, data; lines, fitted curves.

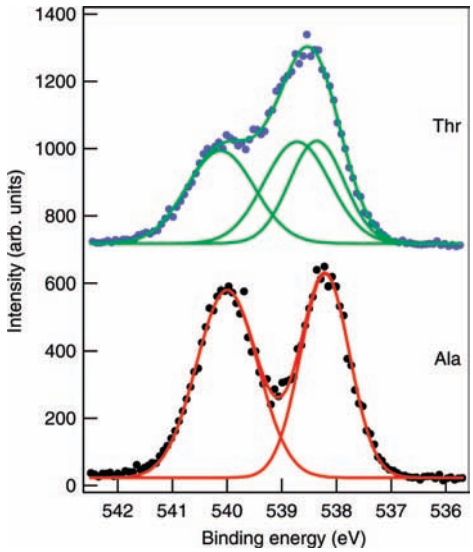

Figure 6. O 1s photoemission spectra of threonine (upper dotted curve) and alanine (lower dotted curve) together with fitted peaks: points, data; lines, fitted curves.

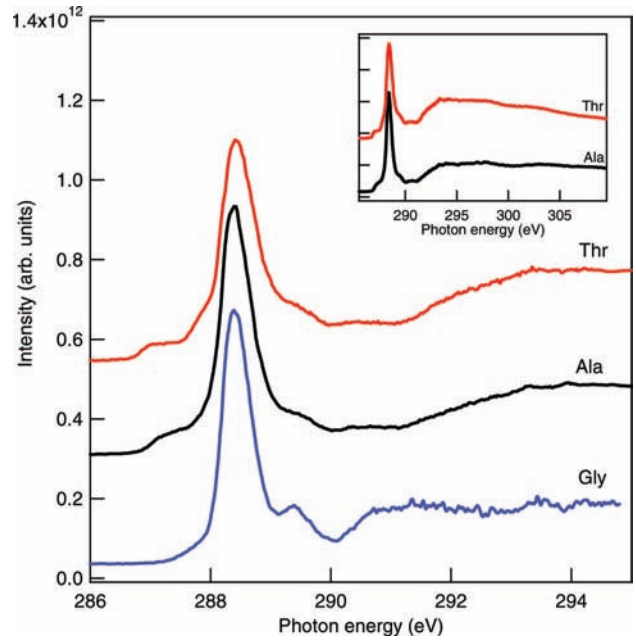

Figure 7. C K-edge NEXAFS spectra of threonine, alanine, and glycine.

rise to an experimental energy difference of 0.5 eV and a theoretical difference of 1.0 eV. We therefore associate the main peak predominantly with conformer I and the minor peak with conformer IIa. We discuss the assignment and quantitative evaluation of the populations further in the Discussion section.

For threonine, the situation is rather complex due to the very large number of possible conformers.[34] However, we may draw the qualitative conclusion that the broadening of the N 1s peak is due to conformer effects. The calculations give a difference of 0.4 eV for the two conformers considered, even though the local hydrogen bonding of the amino group is the same, COH···N, but the hydrogen bonding of O(3) differs. We surmise that conformers in which different classes of hydrogen bonding, such as the NH···O═C conformation considered for alanine, would give even larger shifts.

In Figure 6, the oxygen 1s photoemission spectrum of alanine is very similar to that of glycine, proline, and methionine,[4] while the spectrum of threonine shows additional intensity due to the hydroxyl group O(3). This extra intensity overlaps the peak due to the oxo oxygen of the carboxylic group. The spectrum was fitted with three Gaussian peaks, with energy, width, and intensity as free parameters. We assign the peak fitted at 540.1 eV to the hydroxyl O(2) peak on the basis of the calculation, and there are two peaks due to O(3) and O(1) with binding energies which differ by 0.3 eV. The calculation predicts a difference of about 0.1−0.3 eV, with O(1) at lower binding energy. We assign the components accordingly.

4.3. C, N, and O K-Edge NEXAFS Spectra. Figure 7 presents the C 1s photoabsorption spectra of alanine and threonine, while the experimental and calculated energies of the resonances and proposed assignments are summarized in Table 3. The NEXAFS spectra are very similar to one another, and in Table 3 we compare the data with the simplest amino acid, glycine.[29] The spectra of alanine and threonine show strong, asymmetric peaks at 288.4 eV of width 0.6 eV, assigned to excitations of the carboxylic carbon 1s to the empty π^*(C═O(1)) orbital. The clear shoulder in the alanine spectrum at 287.4 eV is assigned to excitation of methyl carbon Cβ 1s electrons to the vacant σ^*_{CH} orbital on the basis of our calculations, consistent with the solid-state spectra of ref 19. This assignment is however in disagreement with the recent calculations of Jiemchooroj et al. [13] for alanine, who assigned the peak to transitions from Cβ (in our notation) to π^*_{COOH}, i.e., a molecular orbital involving the π system of the carboxylic acid group. We return to this point below in the Discussion section. The shoulder at 287.8 eV in the alanine spectrum is due to excitation of Cα 1s electrons to the vacant σ^*_{CH} orbital.

Threonine also shows two shoulders below the main C 1s → π^* resonance assigned to Cγ 1s transitions to the LUMO and LUMO + 1. As for alanine, these are transitions from methyl C 1s core levels.

A shoulder in the high-energy part of the main peak at about 289.5 eV for both amino acids is assigned to a Cα 1s → σ^*_{CNH} transition and C 1s (side chain) excitations to σ^*_{CH} and σ^*_{CC} states contributing to the oscillator strength in this region.[19] The corresponding sharper peak in the C K-edge NEXAFS spectrum of glycine was centered at 289.4 eV.[29] Jiemchooroj et al.[13] also calculated a pair of states at this energy (relative to the strongest line) for alanine but did not identify them. Further, they calculated that two states existed within an interval of 0.6 eV above the main line with much lower intensity, which may be invisible in the tail of the strong peak. Weak, broad resonances appearing at about 290.6 and 293.3 eV have been attributed to transitions of Cα 1s to σ^*_{CN} + Rydberg and σ^*_{CC}, respectively. The structures observed above the highest IP centered at ~297.8 and ~303 eV are mostly due to shape resonances.[8] In all of these spectra, the conformational effects are calculated to be very small, usually 0.0 or 0.1 eV.

N K-edge NEXAFS spectra are presented in Figure 8, and energies of the resonances and proposed assignments are summarized in Table 4. The nitrogen 1s IPs from the data above are also shown in Table 4. Because the nitrogen local environments are similar in alanine and threonine, the NEXAFS spectra have very similar prominent structures (see Figure 8) and are like glycine.[29] On the basis of our calculations, the assignments are the same for peaks at the same or very similar energies of glycine, as shown in the table.

The first two resonances of alanine at 401.2 and 402.4 eV have widths of about 0.55 and 0.5 eV, respectively; the spectrum is in good overall agreement with published spectra[26–28] but shows better resolved structures (see Table 4). The threonine

TABLE 3: Energies of X-ray Absorption Peaks and Ionization Potentials at the C 1s Edges

molecule	energy (eV)	theoretical energy, (eV) (I−IIa)	assignment	literature values[a] (eV)
alanine	287.4	288.3−288.3	$C\beta$ 1s → σ^*_{CH}	287.6 (s)[19]
	288.4	289.1−289.2	C 1s → $\pi^*_{C=O(1)}$	288.5,[28] 288.5,[26] 288.4 (glycine),[29] 288.6 (s)[18,19]
	289.5	290.0−289.8	$C\alpha$ 1s → σ^*_{CNH} C (side chain) 1s → σ^*_{CH}, σ^*_{CC}	289.4 (glycine),[29] 289.6 (s)[19]
	290.6		$C\alpha$ 1s → σ^*_{CN}+Rydberg	291.3 (glycine),[29] 290.3−291(s)[18]
	293.3		$C\alpha$ 1s → σ^*_{CC}	293.0−297.0 (s)[18]
	297.8		C 1s → $\sigma^*_{C=O(1)}$, shape resonance	
	303.3		shape resonance	
IP, $C\beta$	291.0	291.5−291.8		
IP, $C\alpha$	292.2	293.0−293.3		
IP, $C{=}O(1)$	295.0	296.5−296.1		
threonine	287.2	288.2−288.2 $C\gamma$	$C\gamma$ 1s → σ^*_{CH}	287.6 (s)[19]
	287.8	289.0−289.0 $C\gamma^b$	$C\gamma$ 1s → LUMO + 1	287.7 (glycine)[29]
	288.4	289.2−289.2 C	C 1s → $\pi^*_{C=O(1)}$	288.4 (glycine),[29] 288.6 (s)[19]
	289.5	289.8 −289.9 $C\alpha$	$C\alpha$ 1s → σ^*_{CNH} $C\beta$ 1s → σ^*_{CH}, σ^*_{CC}	289.4 (glycine),[29] 289.3 (s),[19] 289.6 (s)[18]
	290.6	290.4−290.3 $C\beta$	$C\beta$ 1s → σ^*	
	293.4		$C\alpha$ 1s → σ^*_{CC}	293.0−297.0 (s)[18]
	297.8		C 1s → $\sigma^*_{C=O(1)}$, shape resonance	
	302.7		shape resonance	
IP, $C\gamma$	290.8	291.6−291.6		
$IP_{C\alpha}$	292.2	293.2−293.4		
IP, $C\beta$	292.4	293.4−293.3		
IP, $C{=}O(1)$	295.1	296.3−296.5		

[a] The physical state of the sample for literature values is indicated. No indication, alanine in the gas phase; s, solid alanine or threonine; glycine, glycine in the gas phase. [b] Shifted STEX value.

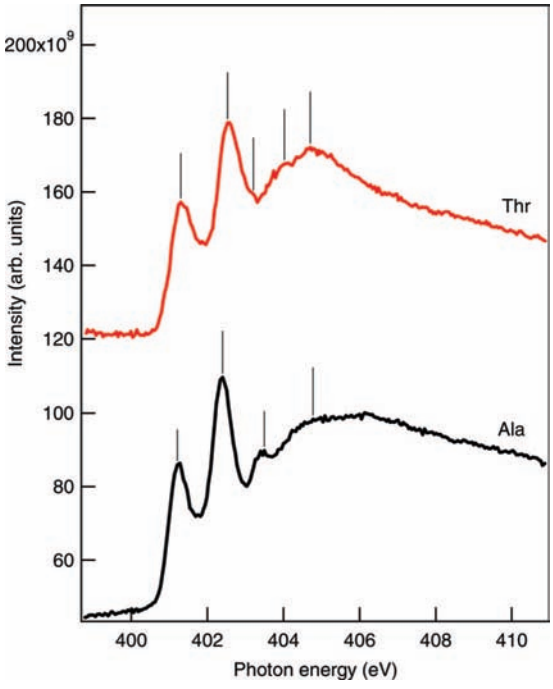

Figure 8. N K-edge NEXAFS spectra of alanine and threonine. Bars mark the positions of resonances.

spectrum shows two peaks at very similar energies to the first two of alanine but are broader (width of >0.6 eV) and more asymmetric. There is a very weak but reproducible feature at 403.2 eV and an unassigned peak at 404.0 eV. The peak at 404.7 eV is assigned to Rydberg states and shape resonances, as for alanine.

In spite of the fact that the N 1s IPs of different conformers show significantly different values, the calculated energies of the transitions in the NEXAFS spectrum show only very small energy differences of up to 0.2 eV for different conformers. This supports our argument based on calculations for proline (above) that conformational effects in NEXAFS are rather small.

The oxygen K-edge spectra of the amino acids are shown in Figure 9, and the energies and proposed assignments of the resonances are summarized in Table 5. The spectrum of alanine resembles glycine,[29] and we make the same assignments as for glycine and formic acid.[53–55] The oxygen K-edge spectrum of alanine is similar to but better resolved than published spectra.[27,28] The first narrower (∼1.0 eV wide) peak at about 532.1 eV for both amino acids is assigned to oxo O(1) 1s transitions to π^* orbitals. The second broader (∼1.5 eV) peak centered at about 535.3 eV is assigned to transitions from hydroxyl O(2) 1s to the same vacant orbital and the mixed 3s/σ^* orbitals. The energy of the third peak matches the energy of the resonances of glycine and formic acid and is assigned to the O(2) 1s → 3p transition.[29,53,54] However, some small differences in the energies of this transition have been observed between formic and amino acids. They appeared at 538.4 eV[53] and 538.3 eV[54] in formic acid and shifted to lower energies, about 537.6 eV, and weakened in the present and previously studied[29] amino acids.

This assignment of the second peak is consistent with the recent calculations of Takahashi et al.[56] and partial ion yield results for formic acid by Tabayashi et al.[57] in which they separated two resonant contributions to the second peak. They assigned the peak to two transitions: O(2) 1s → α^*(CO) and O(2) 1s → σ^*(OH). Our STEX calculations indicate that the two lowest O(2) excitations are close (0.3 eV) and that the second O(2) excitation to the LUMO + 1 is at about the same energy. Thus, our results are in agreement with the DFT calculations of Takahashi et al.[56] that three resonances overlap in this region.

The oxygen K-edge spectrum of threonine also contains structures due to the additional oxygen O(3) in the hydroxyl group, which is assigned on the basis of our calculations and consistent with a previous study of isopropanol near the O 1s threshold.[58] The prominent feature in the threonine spectrum at

TABLE 4: Energies of Peaks and Ionization Potentials at the N 1s Edges

molecule	energy (eV)	theoretical energy, (eV) (I−IIa)	assignment	literature values (eV)
alanine	401.2	402.0−402.1	N 1s → $\sigma^*_{(NH)}$	400.8,[27] 401.0[28]
	402.4	402.9−403.1 403.2	N 1s → $\pi^*_{(NC\alpha)}$ N 1s → σ	401.8,[27] 402.5[28]
	403.5	403.5−403.7	N 1s → $\sigma^*_{(NC\alpha)}$	406.0,[27]
		403.8−403.9	N 1s → π	406.5 (s)[18]
	404.8		Rydberg states, shape resonances	
$IP_{,CF2}$	405.2	405.4 I		405.0[28]
$IP_{,CF1}$	405.9	406.3 IIa		
threonine	401.3	402.3−402.4	N 1s → $\sigma^*_{(NH)}$	
	402.5	403.4−403.4[b]	N 1s → $\pi^*_{(NC\alpha)}$	
	403.2	403.8−403.8[b]	N 1s → $\sigma^*_{(NC\alpha)}$	406.0 (s)[18]
	404.0			
	404.7		Rydberg states, shape resonances	
$IP_{,CF2}$	405.4	406.2 1		
$IP_{,CF1}$	405.9	406.6 2		

[a] The physical state of the sample for literature values is indicated. No indication, alanine in the gas phase; s, solid alanine or threonine; glycine, glycine in the gas phase. CF1 and CF2 are different conformers. [b] Shifted STEX value.

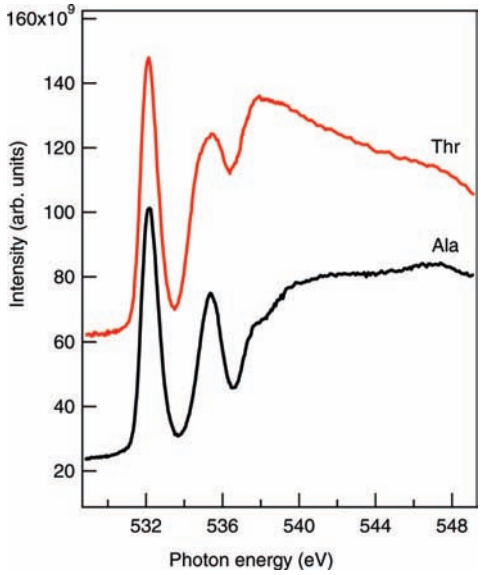

Figure 9. O K-edge NEXAFS spectra of alanine and threonine.

534.4 eV is assigned to the transition of 1s electrons from the hydroxyl (O(3)−H) oxygen to the empty $\sigma^*_{(O(3)-H)}$ orbital. The same transition in the isopropanol spectrum was observed at 0.4 eV lower energy (taking into account the different energy calibration for the calibrant gas). Excitation of O(3) 1s electrons to vacant 3p and $\sigma^*_{(C-O(3))}$ orbitals contributes to weaker structures at about 536.6 and 537.0 eV, respectively.[58] The broad structure above 540 eV observed in both spectra corresponds to σ^* shape resonances associated with the (O(2)−H) and (O(2)−C) single bonds.[25]

Computed transitions involving the O(1) atoms of the carboxylic acid groups do not show appreciable differences in energy between the two conformers considered. However, the O(2) 1s → π^* of alanine shows a considerable shift of 0.9 eV, while the threonine O(3) 1s → σ^* shows a difference of 0.4 eV. This suggests that the large width of the second peak in the spectra is due to not only to the existence of multiple resonances but also hydrogen-bonding-induced shifts, i.e., conformer effects. This appears to be contrary to the trends observed for the other K edges that conformer effects are reduced in photoabsorption compared with photoemission. However, there is no evident reason why this is so.

5. Discussion

The only previous experimental results regarding core level photoemission of the present compounds were published by Powis et al.[5] for alanine, who measured the C 1s binding energies. They obtained energies of 291.2, 292.3, and 295.3 eV as well as a minor peak at 294.15 eV due to polymerization of alanine and formation of a peptide linkage, CONH.[5] These values are consistently higher than ours by about 0.15−0.3 eV. There are several possible reasons for this small discrepancy, of which the most trivial is a difference in calibration (no details were given of the calibration procedure). Their spectra were measured at photon energies of 301 and 309 eV, and postcollision interaction effects may cause small peak shifts and distortion. However, using an estimated hole lifetime of 80 meV we calculate that the shift and peak shape distortion is negligible for the relevant kinetic energies. The photon energies used are in the vicinity of the σ X-ray absorption resonances of alanine, and this may influence the peak shape (non-Franck−Condon effects) and therefore the mean energy. Another possibility is that contaminant peaks other than that observed at 294.15 eV overlapped those of alanine, shifting the energy. Indeed, Powis et al.[5] noted that the Cβ peak, due to ionization of the methyl group, had a "flat-topped" structure which is not the case in our data. This different peak shape as well as the differences in relative peak intensities may have the same causes as the discrepancies in binding energy. Our data do not show evidence of polymerization of alanine, probably because we used a much lower evaporation temperature of 423 K instead of 541 K used by Powis et al.[5] This large difference in temperature probably accounts for the reduced contamination in our spectra. In addition, we did not use a gas cell which tends to trap thermal decomposition products and may catalyze pyrolysis or other chemical changes in thermally labile materials like amino acids.

There appears to be no core level data for threonine in the literature, although Powis et al. tried to evaporate it at 484 K and found that it decomposed. Our lower evaporation temperature of 433 K provided samples without any sign of decomposition.

Regarding NEXAFS, as already mentioned in the Theory Section, the CPP approach[44] provides the total photoabsorption profile but assignment of the individual spectral peaks is not straightforward; in fact, only two of the excitations reported in Figure 2 of ref 13 have been explicitly assigned. While we agree with the comments presented in that paper on the effect of the overscreening in the STEX approximation, also confirmed by our present RAS calculations that provide a correction to that approximation, we find questionable the assignment of both excitations to a transition to an orbital localized on the carboxylic group. Such characterization of the virtual orbital sounds

TABLE 5: Energies of Peaks and Ionization Potentials at the O 1s Edges

molecule	energy (eV)	theoretical energy, (eV) (I−IIa)	assignment	literature values [a]
alanine	532.2	531.7−531.6	O(1) 1s → $\pi^*_{(C=O(1))}$	531.59,[27] 532.0,[28] 532.3−532.5 (s),[18] 533.0 (s)[20]
	535.4	535.7−534.8	O(2) 1s → $\pi^*_{(C=O(1))}$ O(1) 1s → 3s/$\sigma^*_{(O(2)-H)}$ O(2) 1s → 3s/$\sigma^*_{(O(2)-H)}$	534.86,[28] 535.2,[28] 535.2,[28] 536.0 (s),[20] 535.3 (formic acid)[54,55]
	537.6		O(2) 1s → 3p	538.4 (formic acid),[53] 538.3 (formic acid)[54]
IP, $_{(C=O(1))}$	538.2	538.0−537.3		
IP, $_{(O(2)-H)}$	540.0	539.9−539.0		
threonine	532.1	531.6−531.6	O 1s(C═O(1)) → $\pi^*_{(C=O(1))}$	532.3−532.5 (s)[18]
	534.4	534.8−535.2	O 1s(O(3)−H) → $\sigma^*_{(O(3)-H)}$	534 (isopropanol)[58]
	535.4	534.7−534.7	O 1s(O(2)−H) → $\pi^*_{(C=O(1))}$ O 1s(C═O(1)) → 3s/$\sigma^*_{(O(2)-H)}$ O 1s(O(2)−H) → 3s/$\sigma^*_{(O(2)-H)}$	535.8 (formic acid)[57]
	536.6		O 1s(O(3)−H) → 3p	
	537.0		O 1s(O(3)−H) → $\sigma^*_{(C-O(3))}$	
	537.7		O 1s(O(2)−H) → 3p	
IP, $_{(C=O(1))}$	538.4	537.5−537.7		
IP, $_{(O(3)-H)}$	538.7	538.6−538.0		
IP, $_{(O(2)-H)}$	540.1	539.2−539.5		

[a] The physical state of the sample for literature values is indicated. No indication, alanine; s, solid alanine or threonine; glycine, glycine.

reasonable for excitation at the carbonyl C atom but not for that at the methyl C atom. The CPP algorithm is projected on the ground-state orbital set and not on a set of relaxed virtual orbitals reflecting the different localization of the core hole in the different excitation channels. A comparison (not explicitly reported for brevity) of the electron density of the ground-state LUMO with the optimized one deriving from a STEX calculation for excitations at the methyl C atom shows clearly that in the first case the orbital, as actually found in ref 13, looks like a π^* orbital localized on the carboxylic group, while in the second case the LUMO is essentially a σ^* orbital localized along the C_β−H bond. Moreover, the RAS calculation for that excited state shows that such orbital shape is practically not affected by the STEX overscreening. We then find that the label $C_\beta \rightarrow \sigma^*$(CH) better represents the character of that excitation.

One of the most notable results presented here is the broadening of the nitrogen 1s spectra. Figure 10 show the low-resolution alanine spectrum superimposed on the glycine spectrum, and the extra intensity at high binding energy is evident. At higher resolution, Figure 5, the high-energy region appears to be a shoulder rather than a tail. For this reason we believe that the broadening is due to the presence of additional conformers, as discussed above.

As mentioned in the Introduction, Blanco et al.[33] measured the populations of alanine in a jet-cooled beam using microwave spectroscopy. Like in ref 31 they calculated that four conformers were populated at 498 K, observed only two, and explained this by relaxation of two of the conformers during the cooling process in the jet source. The conformers were labeled I (ground state, asymmetric bifurcated $NH_2\cdots O{=}C$ bond), IIa and IIb (second most stable, $OH\cdots NH_2$ bond), and IIIa ($NH\cdots OH$ bond). If we assume that the N core level shifts according to the local hydrogen bonding, then it is unlikely that we can distinguish conformers IIa and IIb spectroscopically because the local chemical environment is very similar. The predicted ratios of the populations at 498 K are 0.68:0.21:0.11 for conformers I, II, and III, respectively. The N 1s binding energy of the type III conformer is likely to be similar to that of conformer I because they are both amino hydrogen donors whereas in II the amino nitrogen is a hydrogen acceptor, giving a predicted ratio of 0.79:0.21. By fitting two peaks to the experimental data, Table 2, we obtain a ratio of 0.78:0.22, in good agreement with the thermochemical prediction of Blanco et al. The assignment of the stronger line to conformers of types I and III and the weaker peak to conformers of type II is consistent with our model calculation that conformer I has lower binding energy.

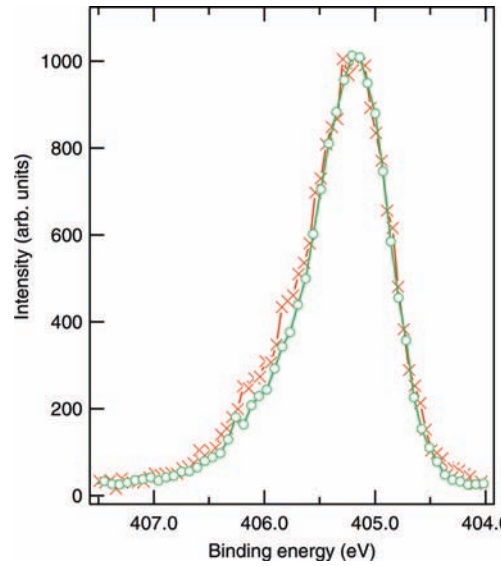

Figure 10. Comparison of the N 1s photoemission spectra of alanine (×) and glycine (○)[4] at the same resolution. The glycine curve has been shifted 0.2 eV to lower binding energy to align the right-hand sides of the two curves.

The threonine N 1s peak is rather broad and does not allow detailed fitting because it is not possible to choose a reasonable number of peaks. Zhang and Lin[34] calculated the populations of conformers in the gas phase, which they list in their Table 5. There are seven conformers with populations above 5% of the total and many more with lower populations. This is because the molecule forms not only the usual structures based on interactions between the amino and carboxylic groups but also conformations in which the additional hydroxyl group interacts with the amino and carboxylic acid groups as either a proton donor or a proton acceptor. The large number of conformers is consistent with at least two broad and unresolved peaks.

6. Conclusions

In this paper we examined the possibility of observing the effect of conformational differences on NEXAFS and core level photoemission spectra. We extended our previous work on proline and carried out new calculations using an economical algorithm on alanine and threonine. The results were compared with experimental results on these compounds. The calculations predict that conformer effects at the C and N 1s edges are much weaker in photoabsorption than in photoemission, which may explain their lack of observation to date. This is due to the fact that the changes in electronic structure due to conformational variation tend to shift both the core and the virtual orbitals by the same energy, so that the energy for X-ray absorption changes very little. Stronger effects are predicted at the O 1s edge, but the spectral features are broader at this edge, making observation difficult.

Acknowledgment. O.P. thanks the Central European Initiative for a fellowship. We thank our colleagues at Elettra for their assistance and providing high-quality synchrotron light.

References and Notes

(1) de Vries, M. S.; Hobza, P. *Annu. Rev. Phys. Chem.* **2007**, *58*, 585.
(2) Slaughter, A. R.; Banna, M. S. *J. Phys. Chem.* **1988**, *92*, 2165.
(3) Plekan, O.; Feyer, V.; Richter, R.; Coreno, M.; de Simone, M.; Prince, K. C.; Carravetta, V. *Chem. Phys. Lett.* **2007**, *442*, 429.
(4) Plekan, O.; Feyer, V.; Richter, R.; Coreno, M.; de Simone, M.; Prince, K. C.; Carravetta, V. *J. Phys. Chem. A* **2007**, *111*, 10998.
(5) Powis, I.; Rennie, E. E.; Hergenhahn, U.; Kugeler, O.; Bussy-Socrate, R. *J. Phys. Chem. A* **2003**, *107*, 25.
(6) Chong, D. P. *Can. J. Chem.* **1996**, *74*, 1005.
(7) Stöhr, J. *NEXAFS Spectroscopy*; Springer: Berlin, 1992.
(8) Plashkevych, O.; Carravetta, V.; Vahtras, O.; Ågren, H. *Chem. Phys.* **1998**, *232*, 49.
(9) Carravetta, V.; Plashkevych, O.; Ågren, H. *J. Chem. Phys.* **1998**, *109*, 1456.
(10) Li, Y.; Plashkevych, O.; Vahtras, O.; Carravetta, V.; Ågren, H. *J. Sync. Radiat.* **1999**, *6*, 708.
(11) Mochizuki, Y.; Ågren, H.; Pettersson, L. G. M.; Carravetta, V. *Chem. Phys. Lett.* **1999**, *309*, 241.
(12) Carravetta, V.; Plashkevych, O.; Ågren, H. *Chem. Phys.* **2001**, *263*, 231.
(13) Jiemchooroj, A.; Ekström, U.; Norman, P. *J. Chem. Phys.* **2007**, *127*, 165104.
(14) Otero, E.; Urquhart, S. G. *J. Phys. Chem. A* **2006**, *110*, 12121.
(15) Zubavichus, Y.; Zharnikov, M.; Schaporenko, A.; Grunze, M. *J. Electron Spectrosc. Relat. Phenom.* **2004**, *134*, 25.
(16) Zubavichus, Y.; Zharnikov, M.; Shaporenko, A.; Fuchs, O.; Weinhardt, L.; Heske, C.; Umbach, E.; Denlinger, J. D.; Grunze, M. *J. Phys. Chem. A* **2004**, *108*, 4557.
(17) Zubavichus, Y.; Fuchs, O.; Weinhardt, L.; Heske, C.; Umbach, E.; Denlinger, J. D.; Grunze, M. *Radiat. Res.* **2004**, *161*, 346.
(18) Zubavichus, Y.; Schaporenko, A.; Grunze, M.; Zharnikov, M. *J. Phys. Chem. A* **2005**, *109*, 6998.
(19) Kaznacheyev, K.; Osanna, A.; Jacobsen, C.; Plashkevych, O.; Vahtras, O.; Ågren, H.; Carravetta, V.; Hitchcock, A. P. *J. Phys. Chem. A* **2002**, *106*, 3153.
(20) Tanaka, M.; Nakagawa, K.; Koketsu, T.; Agui, A.; Yokoya, A. *J. Sync. Radiat.* **2001**, *8*, 1009.
(21) Kaneko, F.; Tanaka, M.; Narita, S.; Kitada, T.; Matsui, T.; Nakagawa, K.; Agui, A.; Fujii, K.; Yokoya, A. *J. Electron Spectrosc. Relat. Phenom.* **2005**, *144*−*147*, 291.
(22) Boese, J.; Osanna, A.; Jacobsen, C.; Kirz, J. *J. Electron Spectrosc. Relat. Phenom.* **1997**, *85*, 9.
(23) Messer, B. M.; Cappa, C. D.; Smith, J. D.; Drisdell, W. S.; Schwartz, C. P.; Cohen, R. C.; Saykally, R. J. *J. Phys. Chem. B* **2005**, *109*, 21640.
(24) Messer, B. M.; Cappa, C. D.; Smith, J. D.; Wilson, K. R.; Gilles, M. K.; Cohen, R. C.; Saykally, R. J. *J. Phys. Chem. B* **2005**, *109*, 5375.
(25) Gordon, M. L.; Cooper, G.; Morin, C.; Araki, T.; Turci, C. C.; Kaznatcheev, K.; Hitchcock, A. P. *J. Phys. Chem. A* **2003**, *107*, 6144.
(26) Cooper, G.; Gordon, M.; Tulumello, D.; Turci, C.; Kaznatcheev, K.; Hitchcock, A. P. *J. Electron Spectrosc. Relat. Phenom.* **2004**, *137*−*140*, 795. See also: http://unicorn.mcmaster.ca/corex/cedb-title.html.
(27) Marinho, R. R. T.; Lago, A. F.; Homem, M. G. P.; Coutinho, L. H.; de Souza, G. G. B.; Naves de Brito, A. *Chem. Phys.* **2006**, *324*, 420.
(28) Morita, M.; Mori, M.; Sunami, T.; Yoshida, H.; Hiraya, A. *Chem. Phys. Lett.* **2006**, *417*, 246.
(29) Plekan, O.; Feyer, V.; Richter, R.; Coreno, M.; de Simone, M.; Prince, K. C.; Carravetta, V. *J. Electron Spectrosc. Relat. Phenom.* **2007**, *155*, 47.
(30) Nolting, D.; Aziz, E. F.; Ottosson, N.; Faubel, M.; Hertel, I. V.; Winter, B. *J. Am. Chem. Soc.* **2007**, *129*, 14068.
(31) Stepanian, S. G.; Reva, I. D.; Radchenko, E. D.; Adamowicz, L. *J. Phys. Chem. A* **1998**, *102*, 4623.
(32) Linder, R.; Seefeld, K.; Vavra, A.; Kleinermanns, K. *Chem. Phys. Lett.* **2005**, *409*, 260.
(33) Blanco, S.; Lesarri, A.; Lopez, J. C.; Alonso, J. L. *J. Am. Chem. Soc.* **2004**, *126*, 11675.
(34) Zhang, M.; Lin, Z. *J. Mol. Struct.: Theochem* **2006**, *760*, 159.
(35) Stepanian, S. G.; Reva, I. D.; Radchenko, E. D.; Adamowicz, L. *J. Phys. Chem. A* **2001**, *105*, 10664.
(36) Prince, K. C.; Blyth, R. R.; Delaunay, R.; Zitnik, M.; Krempasky, J.; Slezak, J.; Camilloni, R.; Avaldi, L.; Coreno, M.; Stefani, G.; Furlani, C.; de Simone, M.; Stranges, S. *J. Sync. Rad.* **1998**, *5*, 565.
(37) Myrseth, V.; Bozek, J. D.; Kukk, E.; Sæthre, L. J.; Thomas, T. D. *J. Electron Spectrosc. Relat. Phenom.* **2002**, *122*, 57.
(38) Thomas, T. D.; Shaw, R. W., Jr. *J. Electron Spectrosc. Relat. Phenom.* **1974**, *5*, 1081.
(39) Hatamoto, T.; Matsumoto, M.; Liu, X.-J.; Ueda, K.; Hoshino, M.; Nakagawa, K.; Tanaka, T.; Tanaka, H.; Ehara, M.; Tamaki, R.; Nakatsuji, H. *J. Electron Spectrosc. Relat. Phenom.* **2007**, *155*, 54.
(40) Tronc, M.; King, G. C.; Read, F. H. *J. Phys. B: At. Mol. Phys.* **1979**, *12*, 137. *J. Phys. B: At. Mol. Phys.* **1980**, *13*, 999.
(41) Sodhi, R. N. S.; Brion, C. E. *J. Electron Spectrosc. Relat. Phenom.* **1984**, *34*, 363.
(42) Wight, G. R.; Brion, C. E. *J. Electron Spectrosc. Relat. Phenom.* **1974**, *3*, 191.
(43) Cannington, P. H.; Ham, N. S. *J. Electron Spectrosc. Relat. Phenom.* **1979**, *15*, 79 Cannington, P.H.; Ham, N.S. *J. Electron Spectrosc. Relat. Phenom.* **1983**, *32*, 139.
(44) Ekström, U.; Norman, P.; Carravetta, V.; Ägren, H. *Phys. Rev. Lett.* **2006**, *97*, 143001.
(45) Flores-Moreno, R.; Zakrzewski, V. G.; Ortiz, J. V. *J. Chem. Phys.* **2007**, *127*, 134106.
(46) DALTON, a molecular electronic structure program, Release 2.0 (2005), see \\http://www.kjemi.uio.no/software/dalton/dalton.html.
(47) Becke, A. D. J. *Chem. Phys.* **1993**, *98*, 5648–5652.
(48) Lee, C. T.; Yang, W. T.; Parr, R. G. *Phys. Rev. B* **1988**, *37*, 785.
(49) Schmidt, M. W.; Baldridge, K. K.; Boatz, J. A.; Elbert, S. T.; Gordon, M. S.; Jensen, J. J.; Koseki, S.; Matsunaga, N.; Nguyen, K. A.; Su, S.; Windus, T. L.; Dupuis, M.; Montgomery, J. A. *J. Comput. Chem.* **1993**, *14*, 1347.
(50) Dunning, T. H. *J. Chem. Phys.* **1971**, *55*, 716.
(51) Schafer, A.; Horn, H.; Ahlrichs, R. *J. Chem. Phys.* **1992**, *97*, 2571.
(52) Ägren, H.; Carravetta, V.; Vahtras, O.; Pettersson, L. G. M. *Theor. Chim. Acc.* **1997**, *97*, 14.
(53) Di Tommaso, D.; Decleva, P. *J. Chem. Phys.* **2005**, *123*, 064311.
(54) Prince, K. C.; Richter, R.; de Simone, M.; Coreno, M. *J. Phys. Chem. A* **2003**, *107*, 1955.
(55) Ishii, I.; Hitchcock, A. P. *J. Chem. Phys.* **1987**, *87*, 830.
(56) Hergenhahn, U.; Rüdel, A.; Maier, K.; Bradshaw, A. M.; Fink, R. F.; Wen, A. T. *Chem. Phys.* **2003**, *289*, 57.
(57) Takahashi, O.; Yamanouchi, S.; Yamamoto, K.; Tabayashi, K. *Chem. Phys. Lett.* **2006**, *419*, 501–505.
(58) Tabayashi, K.; Yamamoto, K.; Takahashi, O.; Tamenori, Y.; Harries, J. R.; Gejo, T.; Iseda, M.; Tamura, T.; Honma, K.; Suzuki, I. H.; Nagaoka, S.; Ibuki, T. *J. Chem. Phys.* **2006**, *125*, 194307.
(59) Thomas, M. K.; Hatherly, P. A.; Codling, K.; Stankiewicz, M.; Rius, J.; Karawajczyk, A.; Roper, M. *J. Phys.B: At. Mol. Opt. Phys.* **1998**, *31*, 3407.
(60) Lesarri, A.; Mata, S.; Cocinero, E. J.; Blanco, S.; Lopez, J. C.; Alonso, J. L. *Angew. Chem., Int. Ed.* **2002**, *41*, 4673.
(61) Allen, W. D.; Czinki, E.; Császár, A. G. *Chem. Eur. J.* **2004**, *10*, 4512.

JP803017Y